

NRC Publications Archive Archives des publications du CNRC

Laser assisted cold spray for improved adhesion of soft materials on hard substrates: case study for copper coatings on steel

Legoux, Jean-Gabriel; Guerreiro, Bruno; Poirier, Dominique; Giallonardo, Jason D.

This publication could be one of several versions: author's original, accepted manuscript or the publisher's version. /
La version de cette publication peut être l'une des suivantes : la version prépublication de l'auteur, la version acceptée du manuscrit ou la version de l'éditeur.

Publisher's version / Version de l'éditeur:

International Thermal Spray Conference (ITSC), Québec City, Canada, May 24-27, 2021, 2021-05-24

NRC Publications Archive Record / Notice des Archives des publications du CNRC :

<https://nrc-publications.canada.ca/eng/view/object/?id=fa4d9286-9ab8-4dc2-9a1c-1af208ff6b02>

<https://publications-cnrc.canada.ca/fra/voir/objet/?id=fa4d9286-9ab8-4dc2-9a1c-1af208ff6b02>

Access and use of this website and the material on it are subject to the Terms and Conditions set forth at

<https://nrc-publications.canada.ca/eng/copyright>

READ THESE TERMS AND CONDITIONS CAREFULLY BEFORE USING THIS WEBSITE.

L'accès à ce site Web et l'utilisation de son contenu sont assujettis aux conditions présentées dans le site

<https://publications-cnrc.canada.ca/fra/droits>

LISEZ CES CONDITIONS ATTENTIVEMENT AVANT D'UTILISER CE SITE WEB.

Questions? Contact the NRC Publications Archive team at

PublicationsArchive-ArchivesPublications@nrc-cnrc.gc.ca. If you wish to email the authors directly, please see the first page of the publication for their contact information.

Vous avez des questions? Nous pouvons vous aider. Pour communiquer directement avec un auteur, consultez la première page de la revue dans laquelle son article a été publié afin de trouver ses coordonnées. Si vous n'arrivez pas à les repérer, communiquez avec nous à PublicationsArchive-ArchivesPublications@nrc-cnrc.gc.ca.

Laser Assisted Cold Spray for Improved Adhesion of Soft Materials on Hard Substrates: Case Study for Copper Coatings on Steel

Jean-Gabriel Legoux, Bruno Guerreiro, Dominique Poirier
National Research Council of Canada (NRC), Boucherville, QC, Canada

Jason D. Giallonardo
Nuclear Waste Management Organization (NWMO), Toronto, ON, Canada

Abstract

In cold spray, high adhesion of soft materials on hard substrates is commonly achieved by using helium as the propelling gas. This is the case of copper coatings on steel where adhesion may reach values as high as 60 to 80 MPa (glue failure); however, helium is a limited, expensive natural resource, and the use of more abundant nitrogen gas is preferred in an industrial setting. Unfortunately, when using nitrogen gas, little to no adhesion is obtained. In order to eliminate the use of helium gas we studied how laser assisted cold spray could lead to an improvement in adhesion of nitrogen sprayed copper coatings. In this work, several laser parameters (e.g., power and spot size) and process parameters (traverse speed, relative position laser spot vs. gas jet) were varied at a coupon level. Upon optimization, an equivalent adhesion to the coatings prepared with helium was obtained. Furthermore, the cross section of the coatings showed that the copper particles penetrated the steel, similar to what is observed when using helium gas. Optimization of these parameters for application to large diameter (~559 mm) cylinders was also performed. A discussion on the mechanisms which contribute to achieving high adhesion considering the use of helium versus laser assistance is provided.

Introduction

In cold spray, as for any coating process, the properties of a coating are dictated by the properties of the materials involved and the process parameters. In particular, the coating adhesion will depend on the properties of the interface between the coating and the substrate it is deposited on. In some cases, the composition of the coating and substrate is the same, and in such a case the main differences between the adhesion and the cohesion of the coating is the material state during the incoming particle impact. For dissimilar materials, the nature of both materials plays an important role. The quality of interfaces can be influenced by many factors, such as surface properties of the incoming particles, the surface nature of the pre-deposited particles and the surface properties of the substrate [1]. The process parameters control mostly the inflight particle properties (temperature and velocity) as well as the temperature and state of either the substrate or the pre-deposited material [2]. Of course, the mechanical properties of the substrate play an important role in the adhesion mechanism involved in the cold spray process. Deformation on both sides of the interface

between an impinging particle and the substrate is of prime importance in order to achieve high adhesion [3]. Experimental conditions are required to ensure that the critical velocity can be reached in order to activate deformation based interactions between the two surfaces such as adiabatic shear instability [4] or hydrodynamic plasticity [5]. Two types of adhesion mechanisms have been identified for cold spray coatings, namely (i) mechanical anchoring of the impinging particles, and (ii) particle penetration into the substrate. The mechanical anchoring mechanism is dependent on the surface roughness that can be created on the hard material side. This mechanism was as demonstrated in the work T. Klassen [6] and of B. Jodoin's team where an increase in substrate roughness was achieved by pulsed water jet system and resulted in high adhesion when using relatively low velocity cold spray system [7]. Physically based simulations have been applied using these concepts [7]. Alternatively, high adhesion can be attained by promoting high particle penetration either by increasing the particle velocity or by softening the substrate. One way, in particular, to increase particle velocity is to use helium as the accelerating gas. Because of its low density, He gas is able to propel the particles faster when compared to nitrogen gas, e.g. [9-10]. This is the case of copper coatings on steel where adhesion may reach values as high as 60 to 80 MPa (glue failure) when prepared with He; however, helium is a limited, expensive natural resource, and the use of more abundant nitrogen gas is preferred in an industrial setting. Another way of ensuring a good deformation of the substrate is to soften it. Surface temperature has been shown to play an important role in coatings properties [11]. Probably the most traditional way of doing so is to heat the material. In the case of steel, the mechanical properties decrease by about 50% at temperature as low as 500°C [12]. One way of doing so in a dynamic regime like atmospheric cold spray is to use a fiber laser. The fiber laser can be targeted in the area or close to the area where the coating is being formed.

In this work we explored the potential use of laser assisted cold spray for achieving high adhesion of copper coatings on steel using nitrogen as the carrier gas. This paper aims at describing the experimental optimization process and results leading to the development of a bond layer by using laser assisted cold spray. Particular emphasis is directed at the application of this technique to the used (nuclear) fuel container designed and developed by the Nuclear Waste Management Organization (NWMO) in Canada [13-14]. In this case, copper coatings

specifically serve to provide corrosion protection of the container under deep geological conditions. The implementation of a He free alternative to apply the bond layer would provide for a more cost-effective process in a production environment.

Experimental

Powder

A spherical powder with purity higher than 99.9% and size ranging from $D_{01} > 5\mu\text{m}$ and $D_{90} < 60\mu\text{m}$ from 5N+ (Ville St. Laurent, QC) was used for this study. Typical powder size distribution and chemical composition can be found in Figure 1 and Table 1, respectively. In order to avoid oxidation of the powder, the powder was stored in an inert atmosphere and once opened, preserved under nitrogen atmosphere.

Table 1. Powder composition.

Element	Composition
Cu (%)	>99.95
P (ppm)	<6
S (ppm)	<5
C (ppm)	<20
H(ppm)	<5
O(ppm)	<230

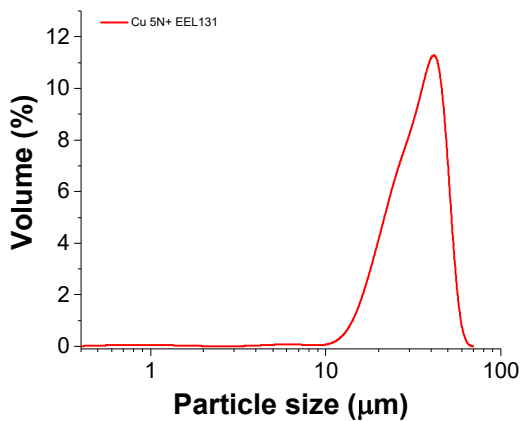


Figure 1. Particle size distribution as measured by laser diffraction.

Substrate

Coatings were prepared on three types of substrates: mild steel plates (7.5 cm vs \times 7.5 cm \times 0.3 cm), 2.54 cm diameter steel pucks (ASTM A36 or equivalent) and on ASTM A106 Gr. C cylinders (~610 mm long, ~559 mm outer diameter and ~457 mm inner diameter). The cylinders are of a similar diameter and wall thickness as compared to the prototype design of the used (nuclear) fuel container developed by the Nuclear Waste Management Organization (NWMO) in Canada, the main difference being that it is shorter and thus, easier to handle.

Coating preparation

In general, the coatings were prepared on grit blasted steel substrates giving Ra values typically between 3 and $6\mu\text{m}$, except for the cylinders for which the surface was cleaned with an automated system using a rotatory abrasion pad (Dynabrade 13204 Dynastraight Finishing Tool) giving Ra values typically between 1 and $2.5\mu\text{m}$. Dimensions of the substrate varied according to the aim of the experiment and are specified in each corresponding section. A PCS-800 cold spray system from Plasma Giken Co. (Yorii-machi, Saitama, Japan) was used as cold spray gun. Spray conditions have been defined earlier [9-10] and have been kept constant in this study. Coatings were prepared in two steps: (i) first a bond layer was sprayed with laser assisted cold spray and (ii) coating buildup was achieved to desired thickness without the use of laser. Nitrogen was used as the carrier gas throughout this work at 800°C and 4.9 MPa.

Laser positioning

In this work, several laser parameters (e.g., power and spot size) and process parameters (traverse speed, relative position laser spot vs. powder jet) were varied.

Figure 2 shows the experimental setup used to control the laser position, with two perpendicular motorized axes, a laser collimator and an optical pyrometer. The laser beam is directed to the particle impact vicinity at an angle of approximately 45° .

As it will be shown in this paper, the precise positioning of the laser beam relatively to the particle jet is of prime importance to control the adhesion of the coatings. Figure 3 shows the traces of the copper particle jet and the laser beam when stopped for a few seconds at the surface of a steel plate. The circular shape of the particle jet and the elliptical shape of the laser beam are recognizable; however, their relative position is difficult to measure precisely. In order to investigate in more detail the effect of the relative position of the particle jet and the laser beam, the positioning of the laser beam centre is described relatively to the particle jet centre as cartesian coordinates (X,Y) in mm. By convention the main gun movement direction is referred to as the X direction and the step direction as the Y direction.



Figure 2. Experimental setup showing the mounted spray gun and laser apparatus on the robot arm.

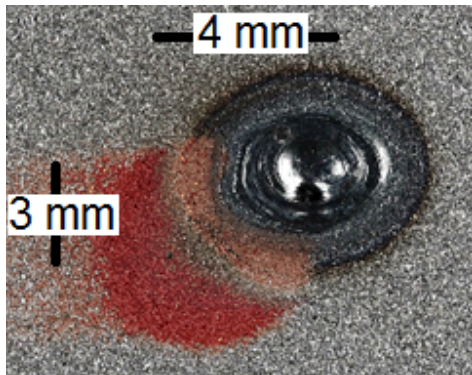


Figure 3. Positioning of the particle jet and laser beam (corresponding to approximately (4,3) in mm, (0,0) being the center of the particle jet).

In order to improve the positioning of the particle jet and the laser beam, laser pointers were added to the setup, one centred on the nozzle exit of the cold spray gun and the other one centred on the laser beam. Figure 4 shows the two spots of the laser pointers for which the distances can easily be measured.

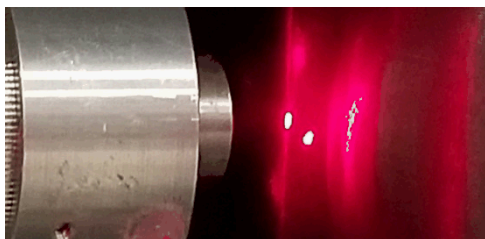


Figure 4. Positioning of the two spots of the laser pointers (diode laser on the spray gun and an aiming laser).

In order to visualize the positioning of the particle jet and the laser beam, two perpendicular lines of coating can be sprayed. The traces left on the plate illustrate the positioning of the two beams and are shown in Figure 5. On the vertical trace, it can be seen that the laser is located to the right of the particle jet while on the horizontal trace, it can be seen that the laser is

located slightly below the particle jet. The traces were made with conditions where the laser was positioned at (7,-2) coordinates, the origin being the centre of the particle jet.



Figure 5. Example of resulting coating corresponding to laser/particle jet positioning (7,-2).

Screening tests

The first series of tests were used for screening purposes regarding laser power, relative positioning of particle jet vs. laser beam and step size. These experiments were performed on 7.5 cm vs × 7.5 cm × 0.3 cm mild steel plates. Traces of ~1 mm thick coatings were produced and then the plate was submitted to bending using a bench vise and a grip. Samples were first bent ~45° and finally ~90°. The results obtained from these experiments were intended to qualitatively assess adhesion with the purpose of defining the starting parameters for the quantitative experiments.

Coupon level adhesion testing

Pull test samples were produced from a flat panel configuration. The 6 pull test samples (per condition) were inserted into a holder made of 3.8 cm thick mild steel panel. The size of the holder was designed so its mass is representative of a large sample. The first layer of the coating was made with laser assistance. In order to guarantee that the particle jet always precedes the laser beam, the bond layer was prepared by moving the laser and the spray gun from left to right while the spray gun and the laser were on the substrate, and coming back to the left side of the holder by making a contour around the holder periphery, as illustrated in Fig. 6. The left to right movement was then resumed with its position shifted by the size of the step to be imposed.

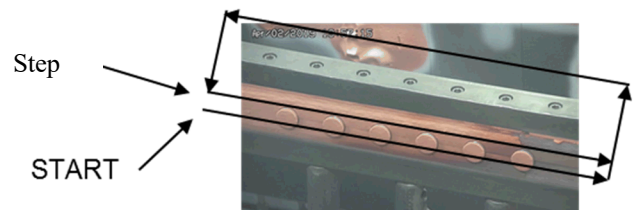


Figure 6. Schematic of the gun path ensuring that the laser beam always precedes the particle jet.

Cylindrical samples

Based on the results obtained on flat surfaces, coatings were produced on short cylinders of 560 mm in diameter and 500 mm in length, with ~40 mm wall thickness

Cylindrical samples were sprayed having the substrate rotate while the spray gun (and laser when applicable) moved linearly and continuously. Two main factors need to be taken into account when transferring the parameters from a flat substrate to a cylindrical one, namely: (i) the gun velocity has to be transformed into the tangential velocity of the cylinder and (ii) the step size needs to be transformed into the gun displacement during one rotation. The tangential velocity, v_{tg} , is given by: $v_{tg} = \pi D(rpm)$, where D is the cylinder’s diameter (560 mm) and rpm is the number of rotations per minute. Velocities were tested around the reference velocity defined in previous section, i.e. 94 mm/s and 126 mm/s, and then tested for rotational speed of 3 and 4 RPM respectively.

The step size of 2 mm was used for the coating of coupons; the equivalent gun traverse speed in order to have 2 mm step with the cylinder had to be determined. Using NRC’s current equipment, the robot speed is limited to 0.1 mm/s increment. When the cylinder is rotating at 3 RPM, this means that it completes one single rotation in 20 s. If the robot speed is 0.1 mm/s, then in 20 s the gun would had moved 2 mm, equivalent to the step used at coupon level. Hence, the required robot velocities in order to have equivalent step sizes of 2, 4 and 6 mm are 0.1, 0.2, 0.3 mm/s, respectively.

A total of six 2.54 cm diameter pull test specimens per condition were extracted from the short cylinder using a hole saw tool. One of the specimens was used for metallographic examination. Adhesion testing was performed in accordance with the ASTM C633 standard procedure.

Results and Discussion

Screening tests

The screening tests were performed in four steps, namely, the determination of laser power, laser/particle jet relative positioning, the step size and the determination of laser optimal laser power. The results are summarized in Table 2, along with the experimental conditions.

The first set of experiments were performed to determine the level of laser power required to maximize adhesion strength. It was performed with the laser beam and the particle jet superposed. Figure 7 shows an example of the appearance of two tested bands after bending. The coating produced with the laser superposed to the particle jet exhibits self debonding, indicating a low adhesion, while coatings B2 to B4 (in Table 2) show cracking followed by debonding at low bend angle for the 2 kW laser power (B2) and at 45° for 3 and 4 kW (B3 and B4). Qualitatively, it is clear that the coatings prepared without laser or at low laser power exhibit lower adhesion strength. From Table 2 it can be seen that samples produced with a laser power of 3 and 4 kW (samples B3 and B4) were less prone to

debonding than the other tested conditions; however, all the experimental conditions with the laser beam superposed to the particle jet resulted in debonding upon bending. Understanding this requires a closer examination of the laser-matter interaction under the particle jet. The steel substrate absorbs relatively well the laser energy (40% absorption coefficient) and thus, can heat up efficiently under the energy flux, compared to copper with an absorption coefficient between 3 and 10% [1]. As the cold spray gun traverses the substrate surface, copper particles impact the steel surface starting practically at the leading edge of the particle jet and gradually covering the entire surface. Eventually copper particles start to pile up and a relatively thick layer of copper is formed. As a result, when the laser beam and particle jet are superposed, the laser beam will hit at least a partially copper covered steel surface and at the same time some copper particles will hit the steel surface prior to the laser beam. In this situation, their impact conditions cannot be optimized in terms of surface temperature. Consequently, in order to maximize the effect of the laser, it is hypothesis that one has to make sure that its energy is absorbed by the steel just prior to the impact of the copper particles. Also, when producing a coating only a small portion of the substrate surface is covered by impacting particles. This newly covered surface is determined by the step size of the raster movement of the gun. Thus, it is this new surface that needs to be heated. Samples B5 to B13 were produced while varying the relative position from 2 to 6 in the X direction and 1 to 5 in the Y direction. All the samples except B5 (with an X relative position of 2 mm) show the formation of cracks on bending without debonding indicating better adhesion than when superposing particles and laser.

Table 2. Results of screening tests, including the laser parameters such as positioning relative to the particles jet and power, and robot parameters such as step size. Traverse speed was constant and equal to 100 mm/s. Coatings were ~1 mm thick.

ID	Positioning		Power	Step size	Comment
	X(mm)	Y(mm)	kW	mm	
Varying the power					
B1	0	0	0	n.a.	Self debonding
B2	0	0	2	n.a.	Debonding at 10°
B3	0	0	3	n.a.	Debonding at 45°
B4	0	0	4	n.a.	Debonding at 45°
Varying relative position					
B5	2	0	3	n.a.	Debonding at 90°
B6	4	0	3	n.a.	Cracks but no Debonding
B7	6	0	3	n.a.	Cracks but no Debonding
B8	8	0	3	n.a.	Cracks but no Debonding
B9	6	1	3	2	Less cracks than previous
B10	6	2	3	2	Cracks but no debonding
B11, B15	6	3	3	2	Some cracks but not through full width
B12	6	4	3	2	Some cracks but not through full width

B13	6	5	3	2	Some cracks but not through full width
Varying step size					
B14	6	3	3	1	Some cracks but not through full width
B15, B11	6	3	3	2	Some cracks but not through full width
B16	6	3	3	3	Few cracks
B17	6	3	3	4	One big crack debonding at 45°
B18	6	3	3	5	One big crack debonding between 45 and 90°
B19	6	0	3	5	One crack at 45°; more at 90° with no debonding
Optimizing Power					
B20	6	3	2	2	Debonding at 45°
B21	6	3	3	2	Cracks but no debonding
B22	6	3	4	2	Cracks but no debonding

The effect of the laser power was then lastly re-assessed with optimal parameters determined by the previous bend testing method. Coating B20 produced with low laser power (2 kW) debonding while the ones prepared with 3 kW laser (B21) or 4 kW laser (B22) did not.

From the results above, it was shown that 3 kW and step size around 2 mm would constitute a good starting point for the quantitative coupon level testing. The screening tests also showed the need to offset the position of the laser beam relative to the particle jet, which can be explained by the need for the incoming particles to hit a preheated steel surface. Thus, the laser beam must be in advance of the particle jet with regards to the surface displacement and the step size must be large enough to ensure that fresh steel is always exposed to the laser first.

Coupon level tests

The trends defined in the screening tests were quantified by performing adhesion tests following the ASTM C633 standard procedure. Adhesion values are compared with those obtained using helium as the process gas to establish the bond layer. Step size, power and positioning of the laser were tested. The results are shown in Table 3. Sample H1 and H2 were produced as a baseline comparison using He gas for the bond layer instead of laser-assisted cold spray. These samples displayed (cohesive) glue failure, that is, breakage of the glue leaving the coating intact with the substrate. Using the conditions defined in the screening tests, step size, gun traverse speed and laser position were varied. The step size was varied from 1 to 3 mm (samples S1 to S3) and the highest adhesion was obtained for the largest step. The gun traverse speed was varied from 100 to 300 mm, showing better results for a gun velocity of 100 mm/s. Finally, the laser position was varied from 4 to 8 mm in the X direction and 2 to 3 mm in the Y direction. For this range of variation it can be seen that when the gun is positioned too far in advance of the particle jet X position of 8 mm, a detrimental effect in the adhesion is observed.

Table 3. Adhesion values for different laser position, gun traverse speed and robot step size. All samples were tested in the as-sprayed condition.

ID	Laser position		Laser Power kW	Gun traverse speed mm/s	Step size mm	Adhesion	
	X mm	Y mm				Average MPa	Stdev MPa
Baseline using helium							
H1	n.a.	n.a.	n.a.	300	1	74*	5
Varying the step size							
S1	7	3	3	100	1	13	8
S2	7	3	3	100	2	14	12
S3	7	3	3	100	3	69*	18
Effect of velocity							
S4	4	3	3	100	2	82*	4

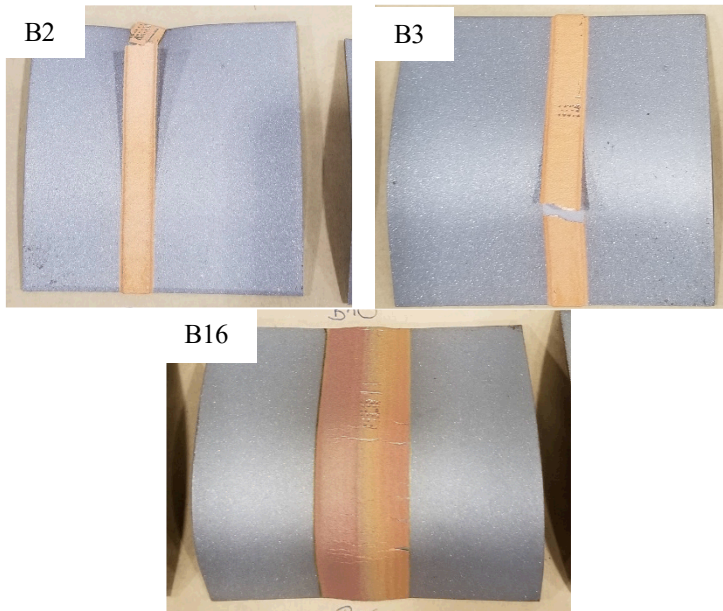


Figure 7. Effect of laser power and positioning after bending at 90°, B2 (2 kW), B3 (4 kW), and B16 (3 kW) located at (6,3) with step size of 3mm.

From the above described results, a relative position of (6,3) seems to offer good potential for further optimization. The effect of the step size was investigated next as shown in samples B14 to B19, where the step was varied from 1 to 5 mm. An attempt was also made to produce the bond layer by depositing adjacent bands with an off centre of (5,0) separated by 5 mm steps (B19 in Table 2). Results for samples B14 through B19 show that samples prepared with large steps of 4 and 5 mm (vs smaller 1-3 mm step sizes) were more prone to debonding. A difference can be noticed between the response of sample B18 [laser position (6,3)] and B19 [laser position (6,0)] where the latter seems to provide higher adhesion strength. It is more efficient to produce adjacent band B19 than having a large precession of the laser B18.

S5	4	3	3	300	2	54	6
Positioning the laser							
S4	4	3	3	100	2	82*	4
S6	7	2	3	100	2	69*	14
S7	8	2	3	100	2	36	26
S8	8	2	3	100	3	26	21

* Glue failure

Cylindrical samples

Finally, trials were performed on cylinders, by varying the robot speed from 0.1 to 0.3 mm/s, laser power from 2 to 4 kW and rotational speed from 3 to 4 rpm. It should be noted that in some applications (e.g., the NWMO used fuel container), coatings require annealing to impart a sufficient level of ductility. Thus, adhesion is further evaluated in both the as-sprayed and post heat treatment (1h, 500°C, Ar). Experimental conditions and resulting adhesion strength are reported in Table 4. The preparation of the bond layer is shown in Figure 8.

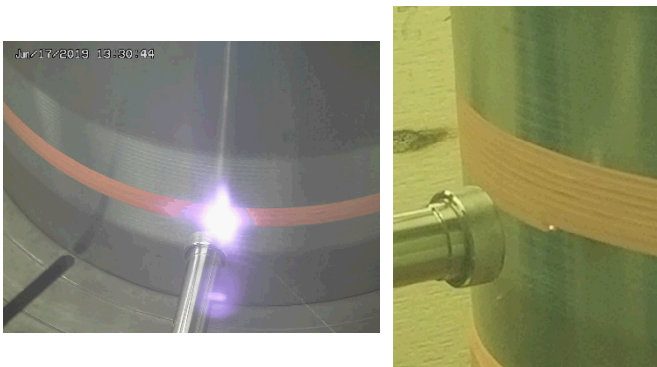


Figure 8. Deposition of the bond layer using laser assistance.

Table 4. Summary of pull tests for various configurations for deposits prepared on short cylinder.

ID	Step size	Surface velocity	Power	Adhesion as-sprayed		Adhesion after HT [2]	
	mm			mm/s	kW	MPa	stdev
Effect of step size							
C1	2	94	3	42	7	84*	2
C2	3	126	4	89*	2	80*	3
C3	4	94	3	57	5	80*	3
C4	6	94	3	25	12	55*	14
Effect of power							
C2	3	126	4	89*	2	80*	3
C3	4	94	3	57	5	80*	3
C5	4	94	3.5	78*	5	78*	9
C6	3	126	4	54	27	86	2
Effect of surface speed							
C2	3	126	4	89*	2	80*	3
C3	4	94	3	57	5	80*	3
C6	3	126	4	54	27	86*	2
Reproducibility at 3.5 kW							
C5	4	94	3.5	78*	5	78*	9
C7	4	94	3.5	n.a.		89*	1

C8	4	94	3.5	87*	2	76*	5
C9	4	94	3.5	n.a.		77*	6
C10	4	94	3.5	n.a.		77*	4
C11	4	94	3.5	n.a.		81*	2
Reproducibility at 3 kW							
C3	4	94	3	57	5	80*	3
C12	4	94	3	36	16	84*	5

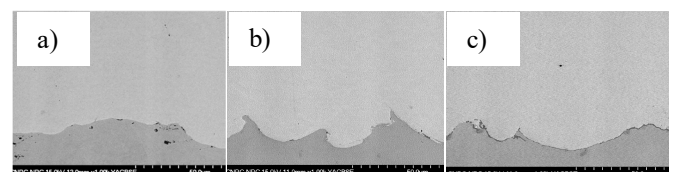
* Glue failure

As shown in Table 4, adhesion values for the as-sprayed condition vary from 25 MPa for an adhesive type failure to 89 MPa with glue failure type. After heat treatment, glue failure was observed for all samples irrespective of the experimental parameters, varying between 55 to 89 MPa. This illustrates the important role of the heat treatment in improving the adhesion values.

In total, twelve spray conditions showed glue failure behaviour after heat treatment, which represents a total of 60 pull studs. Additionally, three conditions C2, C5, C8 also showed glue failure in the as-sprayed condition, representing 15 additional pull studs. Thus, a total of 75 studs displayed glue failure. These results also demonstrate that after heat treatment the adhesion of the cold spray coating deposited with laser assistance is forgiving to experimental variation (namely small variations in laser positioning, on the order of < 1 mm) given that all the tested heat treated coatings exhibited glue failure. Furthermore, from the results obtained in this study it can be noted that in the as-sprayed conditions, more variation with respect to adhesion was observed when using 3 kW laser power. In order to minimize this variation and the risk of overheating the steel substrate, a laser power of 3.5 kW is recommended since it provides consistent adhesion results in both the as-sprayed and heat treated conditions. That is, for the refined or best conditions (laser 3.5 kW, 3 rpm, 0.2 mm/s robot speed) a total of 6 different spray trials (i.e., C5, C7, C8, C9, C10, C11) on short cylinders resulted in glue failure in both the as-sprayed for (C5 and C8) or heat treated conditions for all samples.

Metallographic examination

The resulting (cross-sectional) interfacial areas of the bond layer obtained by laser assistance were compared to that of a helium bond layer. The laser assisted bond layer clearly showed that the copper particles penetrated the steel, similar to what is observed when using helium gas (Figure 9). That is, the interfaces show a deep penetration of the copper particles into the steel surface confirming that there is softening of steel caused by the laser heating. A non-heated surface the surface of the steel would remain unaffected by the impact of copper particles using nitrogen as the carrier gas (Figure 9 d) and e) for a polished and grit blasted surface, respectively).



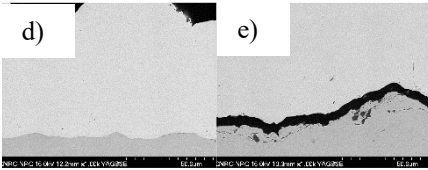


Figure 9. Comparison of the interfacial areas for the different conditions: (a) He bond layer, (b) and (c) laser assisted bond layers at 3.5 kW (3 rpm) and 4 kW (4 rpm), respectively, (d) non-heated interface under N_2 only, polished surface prior to spray (e) non-heated interface under N_2 only, grit blasted surface prior to spray

Conclusions

From this study, the following conclusions can be drawn:

- In order to maximize the efficiency of laser assistance for improving adhesion, the laser beam must be positioned offset to the particle jet on the uncoated substrate surface;
- Optimal results for adhesion are dependent on the laser power and surface velocity;
- Laser assistance enables the ability to attain adhesion levels of soft materials on hard substrates that are above the glue failure strength from ASTM C633 adhesion testing; and,
- Adhesion of copper on steel surfaces is improved by heat treatment.
- Advancement of this technique shows significant promise for use with the NWMO's used (nuclear) fuel containers and similar applications.

References

- [1] Modern Cold Spray; Materials, Process and Applications, Springer, 2015, M. Jeandin, H. Koivuluoto and S. Vezzu, Chapter 4 Coating Properties, pp.107-224.
- [2] Modern Cold Spray; Materials, Process and Applications, Springer, 2015, P.King, M. Yandouzi, B. Jodoin, Chapter 2: The physics of Cold spray, pp.31-67.
- [3] D.Goldbaum, J. M. Shockley, R.R. Chromik, A. Rezaeian, S. Yue, J.G. Legoux and E.Irissou, The Effect of Deposition Conditions on Adhesion Strength of Ti and Ti6Al4V Cold Spray Splats, J. Therm. Spray Technol., 2012, 21(2), p 288-303
- [4] M. Grujicic, C.L. Zhao, W.S. DeRosset, and D. Helfritsch, Adiabatic Shear Instability Based Mechanism for Particles/ Substrate Bonding in the Cold-Gas Dynamic-Spray Process, Mater. Des., 2004, 25(8), p 681-688.
- [5] Mostafa Hassani-Gangaraj, David Veysset, Victor K. Champagne, Keith A. Nelson, Christopher A. Schuh, Adiabatic shear instability is not necessary for adhesion in cold spray in Acta Materiali, Volume 158, 1 October 2018, Pages 430-439
- [6] Stephan Theimer, Martin Graunitz, Matthias Schulze, Frank Gaertner, Thomas Klassen, Optimization Adhesion in Cold Spraying onto Hard Substrates: A Case Study for Brass Coatings, Therm Spray Tech (2019) 28:124-134
- [7] T. Samson, D. MacDonald, R. Fernandez, and B. Jodoin, Adhesion Strength of Cold Gas Dynamic Sprayed Aluminum Coatings, J. Therm. Spray Technol., 2015, 24(6), p 984-993
- [8] Saeed Rahmati I, Bertrand Jodoin, Physically Based Finite Element Modeling Method to Predict Metallic Bonding in Cold Spray, J Therm Spray Tech,
- [9] Bruno Guerreiro, Phuong Vo, Jean-Gabriel Legoux, Xuan Zhang and Jason Giallonardo, Adhesion Strength and Ductility Evaluation of Cold Sprayed Copper Coatings for The Long-term Disposal of Nuclear Fuel, ITSC 2018, Orlando, Florida
- [10] Bruno Guerreiro, Phuong Vo, Dominique Poirier, Jean-Gabriel Legoux, Xuan Zhang, Jason Giallonardo, 'Evaluation of the Ductility of Cold Sprayed Copper Coatings for the Long-Term Disposal of Nuclear Fuel', Proceedings of the International Thermal Spray Conference, 2019-May, pp. 413-419,
- [11] J.G. Legoux, E. Irissou, and C. Moreau, Effect of Substrate Temperature on the Formation Mechanism of Cold-Sprayed Aluminum, Zinc and Tin Coatings, J. Therm. Spray Technol., 2007, 16(5), p 619-626.
- [12] Material Properties of Steel in Fire Conditions, Weiyong Wang, Venkatesh Kodur, Academic Press (Elsevier), 2020 - ch3: Tensile test on steels at elevated temperature, p.43-118
- [13] P. Vo, D. Poirier, J.-G. Legoux, E. Irissou, P.G. Keech, Chapter 10: Application of Copper Coatings onto Used-Fuel Canisters for the Canadian Nuclear Industry in High Pressure Cold Spray, Principles and Applications, ed. C.M. Kay & J. Karthikeyan, ASM International, 2016.
- [14] J.D. Giallonardo, P.G. Keech, and D. Doyle, "Application of Copper Coatings to Used Nuclear Fuel Containers", American Nuclear Society, International High-Level Radioactive Waste Management 2017, Charlotte, NC, April 9-13, 2017, p. 173-182